



A PROBABILISTIC APPROACH TO SPUR GEAR DESIGN FOR CONTACT FATIGUE

Kishan Nath Sidh^a, Yash Chavan^b, and Harish Hirani^{a*}

^a Mechanical Engineering Department, Indian Institute of Technology Delhi, New Delhi 110016, India

^b Department of Mechanical Engineering, BITS Pilani K K Birla Goa Campus, Zuarinagar, Goa 403726, India

* Corresponding Author (Email id: hirani@mech.iitd.ac.in)

ABSTRACT

Classical deterministic gear design approaches (i.e., AGMA, JGMA, FEM) do not incorporate variations in material properties, surface hardness, operating conditions, and geometric tolerances. Often, an analysis is made by considering some misalignment in one of the directions. As a result, over or under design of gear occurs. In the present paper, a design methodology to incorporate uncertainties associated with system input has been proposed and contact fatigue failure of spur gears have been considered. A detailed description of the procedures followed for the AGMA, and the proposed probabilistic approach is presented. The proposed approach is validated against established results obtained through finite element analysis (FEM), providing a more reliable and robust framework for gear design against contact fatigue.

KEYWORDS: AGMA, Statistical variation, Uncertainty, Contact stress, FEM

1. INTRODUCTION

Gears and bearings are critical components in machinery, with their design significantly impacting machine performance. Gears are known for compactness and high transmission efficiency, facilitating power transfer from driving to driven shafts. However, designing these components involves numerous empirical factors, which can complicate achieving designs that are economical, efficient, and capable of handling desired torques with minimal noise and weight.

The challenge in gear design mainly arises from variable factors such as load fluctuations, assembly errors, manufacturing inaccuracies, and changes in operating conditions like temperature, which affect oil viscosity. Traditional design methodologies mostly adopt a deterministic approach, leading to either under or over-design when considering fatigue and

contact stress. With a slight increase (even less than 10%) in loading condition, the fatigue life may reduce up to 50 % [1-2]. Most previous works [3-10] neglected the variations and followed a deterministic approach. The limitation of such deterministic methods points out the inadequacies in addressing real-world variabilities.

The Gaussian distribution is selected to model uncertainties associated with contact fatigue in gear systems, as it is a commonly recommended method in the literature [11]. One of the key advantages of the Gaussian distribution is its well understood statistical properties, which allow for straightforward modeling of random variations in material properties and operating conditions and has the ability to capture variability around a central mean.

Compared to other probabilistic approaches, such as the Weibull and log-normal distributions, the Gaussian distribution provides a balanced approach to modeling uncertainty when variations are symmetrical around a mean value. While Weibull distributions are more suitable for representing life data where failure rates increase over time [12], and log-normal distributions are beneficial for skewed data [13], the Gaussian distribution is appropriate for finding the allowable stress. This choice ensures that our model accurately reflects the typical variations encountered in gear contact fatigue, contributing to a reliable design methodology.

The reliability of gear systems impacts not only on design but also on the manufacturing process, material availability, cost, and the demands of finishing operations. It is crucial to incorporate variations in load, speed, material properties, and manufacturing processes into the design to assess gear reliability [14-19] accurately. Most industry standards, including those from the American Gear Manufacturers Association (AGMA), the Japan Gear Manufacturers Association (JGMA), and the International Standards Organization (ISO), provide guidelines that may not sufficiently account for these complexities related to uncertainty. These standards completely depend on correction factors such as dynamic factor, load distribution factor, and material properties, which may not be universally applicable due to their assumption-based nature.

Andrews [20], Kramberger et al. [21], and Glodez et al. [22] designed the gear to avoid the bending failure of gear teeth. However, it was observed by Gautham et al. [15] that contact factor of safety is more critical than the bending factor of safety.

Though the pitting stress is more than the bending stress in the gear, the allowable endurance contact stress is always several times greater than the contact stress value. So, considering only one type of stress may still result in the failure of gear due to other types of stress.

Recent studies related to this, such as those by Al-Tubi et al. [14], observed 18.5% variation in torque and 13.5% variation in speed in one of typical gearbox used in wind power generators and concluded that these variations in shaft torque and speed contribute to a high risk of gear micro-pitting because of high contact stresses. Li [18] designed gear using ISO standard, JGMA standard and 3D FEM analysis. Li [19] considered machining errors, assembly errors and tooth modification; and concluded that ISO and JGMA standards lack precision in estimating surface contact stress. Using 3D FEM [14,20], the contact stress variations due to several types of errors can be estimated, but this method requires the development of the actual profile of the gear surface and performing 3D FEM is a complicated and time-consuming process. Therefore, there is a need for an alternative method which is easy to implement and considers all the errors related to the gear in operation.

These variations underline the critical need for a design methodology that incorporates statistical variations in design parameters to better reflect real world uncertainties [23-26]. Such an approach would allow gears to be optimally designed, neither under nor over-designed, as illustrated in Figure 1, by considering statistical distributions of stress and endurance strength, thus providing a more reliable prediction of gear failure probabilities.

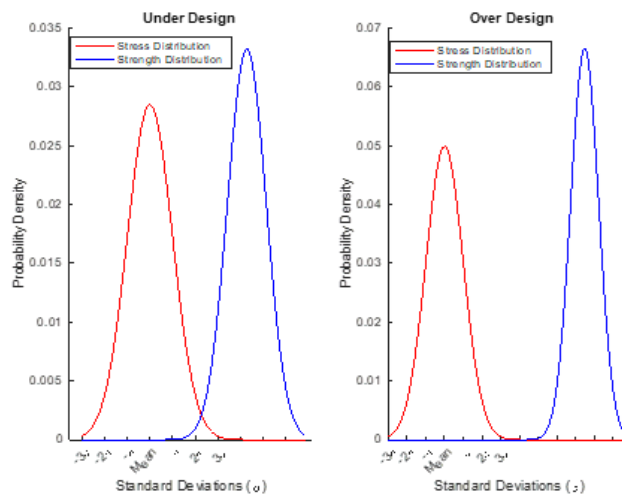


Figure 1. Probability distribution of stress and strength for a) Under design, (b) Over design

This work proposes a probabilistic design methodology that integrates these statistical variations, providing a more robust framework for gear design that reduces reliance on empirical factors and enhances design precision under variable operating conditions. This methodology's effectiveness is illustrated

through a comparative case study with traditional AGMA design approaches, demonstrating its potential applicability to bearing design as well.

2. GEAR DESIGN

Gear designers are required to adhere to the AGMA 2001-D04 standard, which specifies fundamental rating factors and calculation methods for Involute Spur. In this study, we

consider pitting as potential failure modes for spur gears, gear box illustrated in Figure 2. It is essential to evaluate gear safety against pitting types of failures.

2.1 AGMA Approach

The fundamental contact stress Equation used in the classical (AGMA) approach (Budynas and Nisbett, 2014) [26] are given by Equations (1) respectively.

Here, F_t is the transmitted load per unit width, K_o is the overload factor, and factors K_v is the dynamic factor, C_f is Surface finish

factor, K_m is Load distribution factor, and K_s is Size factor. C_p is Elastic coefficient, d is the Operating pitch diameter of pinion, and I is surface geometry factor. The dynamic factor (K_v) is a function of pitch line velocity (V) and manufacturing accuracy. Details for the variables are given in Appendix A.1.

$$\sigma_c = C_p \sqrt{\frac{F_t K_o C_f K_m K_s K_v}{l d}} \quad (1)$$

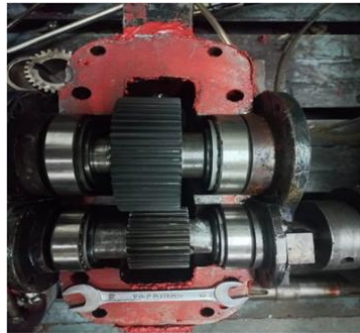


Figure 2. Gear box with spur gear

The elastic coefficient (C_p) is given by,

$$C_p = \sqrt{\frac{1}{\left[\left(\frac{1-\nu_p^2}{E_p}\right) + \left(\frac{1-\nu_g^2}{E_g}\right)\right]}} \quad (2)$$

Where, E_p and E_g are the moduli of elasticity and ν_p and ν_g are the Poisson's ratios for pinion and gear respectively. The surface geometry factor (I) considers the radii of curvature of the gear teeth and the pressure angle. As per AGMA 2001-D04, I given by Equation (3).

$$I = \frac{\sin\phi \cos\phi}{2} \frac{Z_g}{Z_p + Z_g} \quad (3)$$

Where ϕ is the pressure angle, Z_p and Z_g are the number of teeth on pinion and gear, respectively.

In this work, the 3D FEM is used to calculate the contact stress of a pair of spur gears, the parameters of which are listed in Table 4.

Table 4 Parameters of pinion

Sl. No.	Parameter	Pinion	Gear
1	Number of teeth	27	53
2	Pressure Angle (Degree)	20	20
3	Face width (m)	0.033	0.033
5	Torque (Nm)	50.94	100
7	Rotational speed of gear (R.P.M.)	2000	1018.86
10	Youngs Modulus (GPa)	210	
11	Poisson's Ratio	0.3	

To calculate the contact stress using Equation (1), all the required parameters are given in Table 5.

Table 5 The various factors for pitting stress are estimated

Sl. No.	Parameter	Pinion	Gear
2	C_p	191.64	191.64
3	F_t	57.17	57.17
4	K_o	1.5	1.5
5	C_f	1	1
7	K_m	1.12	1.1301
8	K_v	1.1949	1.1949
9	K_s	1.1	1.1
10	I	0.1065	0.1065

Substituting the values of factors in Equation (1) the contact stress found:

- a) Pinion: 898.13 MPa
- b) Gear: 902.13 MPa

The safety factors guarding against pitting (contact failure) (S_{Fc}) are given by Equation (4). To avoid pitting failure, corrected fatigue strength must be satisfied.

$$S_{Fc} = \frac{S_c C_L C_H}{\sigma_c C_T C_R} \quad (4)$$

Where, σ_c are the generated contact stress and S_c is AGMA surface fatigue strength. C_L is the Surface life factor for contact stresses, C_H is the hardness ratio factor, C_T is the temperature factor, and C_R is the reliability factor used to

find the corrected fatigue strength or corrected max allowable contact stress. The value of allowable contact stresses for EN-24 steel is 1250 MPa. The various strength correctness factors are at 10^7 cycles (C_L is 0.907), 99 % reliability (C_R is 1) and temperature up to 121.11°C (C_T is 1.0) for EN-24 steel is given to be when both gear and pinion are of same hardness (C_H is 1). So, the corrected allowable strength will be 1133.75 MPa (using Equation 4). The details of these above discussed factors are given in Appendix A.2. To estimate the factor of safety (FOS) due to pitting stress using the AGMA approach, the values are substituted in Equation (4),

- (i) F.O.S. for Pinion: 1.262
- (ii) F.O.S for Gear: 1.252

2.2 FEM Approach

Simulations were conducted using Ansys, with the material properties detailed in Table 4. The geometric assembly of the gear pair was created in SolidWorks. The analysis focused on an individual gear and pinion tooth rather than the complete gear model to minimize computational expenses. Focusing on

a single tooth provides greater flexibility to analyse the contact region with finer mesh sizes, facilitating a more detailed convergence study. The refined methodology applied for the contact analysis is discussed in detail under the meshing strategy.

To replicate realistic conditions, boundary constraints (as shown in Figure 3(c)) were carefully defined. The root of one gear tooth was fully fixed to restrict all degrees of freedom, while the pinion tooth was assigned a local cylindrical coordinate system centered at the pinion's axis. This allowed the transverse direction to remain free, enabling realistic deformation under loading, while axial and radial directions were fixed to prevent undesired movement. A moment as driving torque 50 Nm was applied to the pinion about its center to simulate torque transmission, for this a local cartesian coordinate system generated at pinion's center.

To ensure accurate results under these conditions, Large Deformation was enabled in the solution settings, accommodating the large displacements caused by the transverse freedom. The contact surfaces were modelled using a frictional contact formulation with a coefficient of friction set to 0.2. The augmented Lagrange method was employed to maintain contact bonding while allowing for slight sliding between surfaces. To compute the contact pressure, a Contact Tool was inserted into the solution settings, and the Pressure result was subsequently extracted from the Contact Tool for further analysis, as illustrated in Figure 3(a) and 3(b).

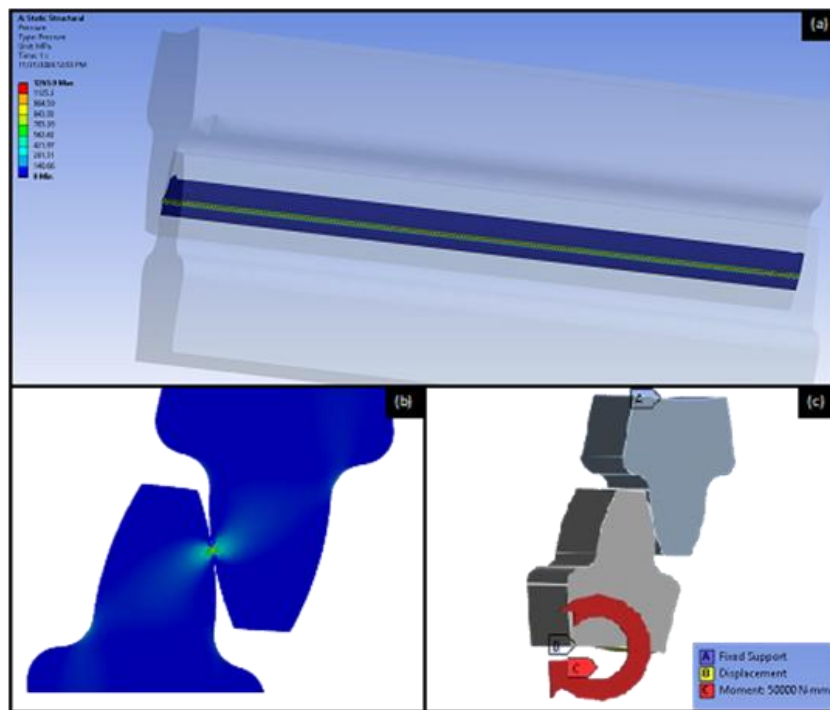


Figure 3. The contact pressure and applied boundary conditions conducted in FEA.

Meshing Strategy

A multi-zone meshing approach was adopted to balance accuracy and computational efficiency. A face split was introduced at the tooth contact region to enable finer control over the mesh resolution. Three distinct mesh sizes were applied across the gear model:

Contact Region: Fine meshes were generated for the split contact face, starting with a mesh size of 1 mm for the first solution. Subsequent solutions refined this size to 0.5 mm, 0.4 mm, 0.3 mm, 0.2 mm, 0.1 mm, and 0.09 mm, progressively increasing resolution for higher accuracy, discussed in Table 6.

Neighboring Faces: The faces adjacent to the contact region were meshed with elements twice the size of those in the contact region to ensure a smooth transition and maintain mesh quality.

Remaining Regions: All other faces were assigned a coarser mesh, with element sizes double those used for the neighboring faces.

The mesh was generated with an aspect ratio of 1:2 to ensure high quality elements throughout the model. The combination of refined mesh sizes and the progressive increase in resolution allowed for capturing the complex contact phenomena while keeping the computational cost manageable.

Table 6 Parameters and results of mesh convergence study

	Contact Pressure (MPa)	Change (%)	Element Size (mm) (at contact region)	Nodes	Elements
1	401.41		1	6450	3426
2	868.63	116.39	0.5	19478	10876
3	1017	17.08	0.4	28510	16144
4	1153.3	13.40	0.3	51074	29208
5	1265.9	9.76	0.2	127650	73754
6	1262.7	-0.25	0.1	507448	296822
7	1270.1	0.58	0.09	624520	365936

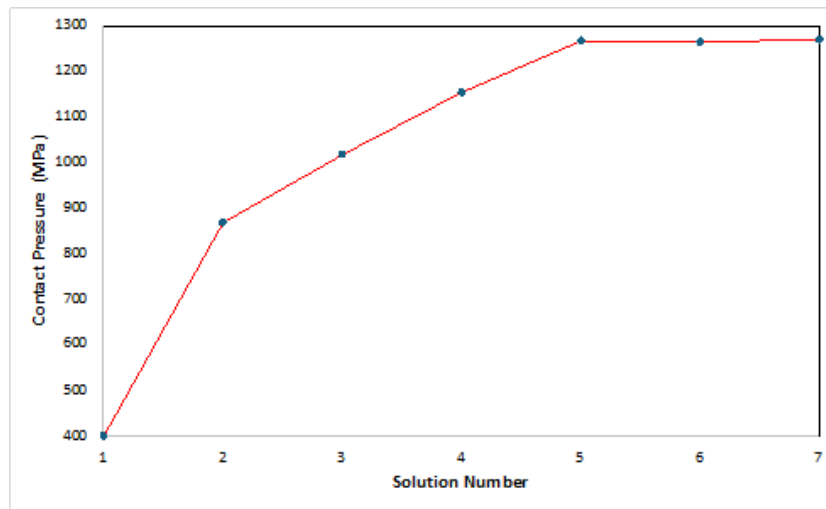


Figure 4. Mesh Convergence Study

The convergence plot exhibits an effective convergence trend (Figure 4). The plot displays a consistent decrease in residuals values, signifying that the solution is progressively improving with each iteration. To balance accuracy and computational efficiency, an element size of 0.2 mm is recommended for fine meshing during contact pressure calculations. Max pressure at the contact region obtained as 1265 MPa. FOS is coming out to be 0.98 for this case.

The results of contact stresses obtained from FEM and AGMA are listed in Table 7. As per the FEM contact stress results, gear will fail by the contact fatigue. The FEM method does not provide a comprehensive procedure as it does not consider several correction factors, which are considered in the AGMA procedure.

Table 7 Contact and Bending stresses

Stresses	AGMA		FEM
	Pinion	Gear	
Contact Stress (MPa)	898.13	902.13	1265
FOS	1.26	1.25	0.98

From the above values it can be observed that, using the AGMA approach, it is predicted that both gear and pinion are safe in pitting condition. As per the FEM result pinion will fail due to contact stresses and will not be able to service even for 10^7 cycles. As there are contradictory results related to contact

fatigue predicted by AGMA and FEM, there is a need to propose a statistical approach that can provide the probability of contact failure.

Proposed Probabilistic Design Approach

The probabilistic method [27-29], which incorporates statistical variations in different design factors, has been developed to address the limitations of traditional approaches. In this approach, it is assumed that the standard

$$f(Q) = \frac{1}{\hat{\sigma}_Q \sqrt{2\pi}} \exp \left[-\frac{1}{2} \left(\frac{Q - \mu_Q}{\hat{\sigma}_Q} \right)^2 \right] \quad (5)$$

Here μ_Q is mean and $\hat{\sigma}_Q$ is standard deviation of the variable concerned. To normalize Equation (5), concept of ‘normal variable’, (Equation 6) having a mean of zero and a standard deviation of unity, can be used.

$$Z = \frac{Q - \mu_Q}{\hat{\sigma}_Q} \quad (6)$$

deviation of each variable follows the Gaussian distribution, such as:

In this method, it is assumed that each variable's standard deviation follows a Gaussian distribution. Figure 5 illustrates the probability distribution curves for stress (σ) and strength (S_y). Failure occurs when the induced stress exceeds the material's strength. The margin of safety (Q) is the difference between the strength and the stress ($Q = S_y - \sigma$). If Q is less than zero, there is a likelihood of failure. Reliability (R), the probability that a component will function without failure, is represented by the area where Q is greater than zero. Conversely, the area of interference ($1 - R$) represents the probability of failure.

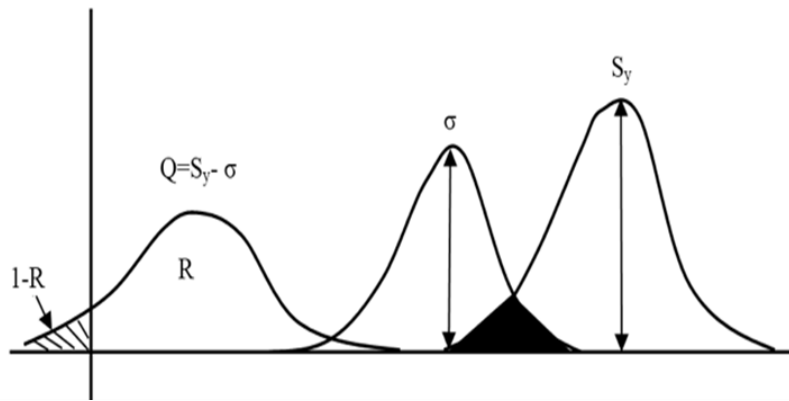


Figure 5. Stress and strength distributions.

To find the chance that $Q > 0$, the value of ‘Z’ variable (Equation 7) is obtained for $Q = 0$.

$$Z = \frac{Q - \mu_Q}{\sigma_Q} = -\frac{\mu_Q}{\sigma_Q} \quad (7)$$

Where $\mu_Q = \mu_S - \mu_\sigma$ and $\sigma_Q = \sqrt{\sigma_S^2 + \sigma_\sigma^2}$. From the value of Z , the reliability of the component is estimated.

In this method, the mean and standard deviation of the stress are determined. The mean stress is computed using the mean values of all design variables. To calculate the standard deviation of stress, the stress Equation is differentiated with respect to each independent variable. Dependent variables are substituted as functions of independent variables where

2.2.1 Contact Stress

Contact stress is influenced by several factors, and uncertainties in these factors accumulate, affecting the overall contact stress calculation [30-32]. The contact stress can be described by Equation (8):

$$\sigma_c = f(C_p, K_v, W_t, F, D, I, K_o, K_s, K_m) \quad (8)$$

In practice, variations in torque and diameter are often measurable, while the load (W_t) is dependent on the applied torque (T) and pitch diameter (D), $f(W_t)$ is replaced by $f(T, D)$. K_v is the function of pitch line velocity (V) (given Equation (A.1)) and V is a function of angular speed (N) and pitch diameter (D). Similarly, the deviation in value of module (m) is almost negligible, so there is no need to consider its standard deviation.

The load distribution factor (K_m) accounts for uneven load sharing between gear teeth due to improper gear and pinion engagement. Errors in gear and pinion assembly, and in the

From the above discussion, Equation (8) is reduced to (9):

$$\sigma_c = f(T, F, D, N, I) \quad (9)$$

Moreover, I is a function of the pressure angle ϕ , as given by Equation (3). The running pressure angle depends on the operating distance between the gear centers. During both assembly and operation, deviations from the nominal gear profile can occur [30], leading to variations in the pitch circle diameter and pressure angle. The pressure angle in the expression for I can be replaced by its instantaneous value,

Equation (9) is rewritten as Equation (10).

$$\sigma_c = f(T, F, D, N, \phi) \quad (10)$$

$$\sigma_c = 191.64 \sqrt{\frac{T f(D, N) f(F, D)}{F D^2 f(\phi)}} \quad (11)$$

$$\sigma_{\sigma_c} = \sqrt{\left(\frac{\partial \sigma_c}{\partial D}\right)^2 \sigma_D^2 + \left(\frac{\partial \sigma_c}{\partial T}\right)^2 \sigma_T^2 + \left(\frac{\partial \sigma_c}{\partial F}\right)^2 \sigma_F^2 + \left(\frac{\partial \sigma_c}{\partial N}\right)^2 \sigma_N^2 + \left(\frac{\partial \sigma_c}{\partial \phi}\right)^2 \sigma_\phi^2} \quad (12)$$

necessary. The contact stress can be examined using Equation (1) for clarity.

mounting of bearings, cause the effective face width in contact to decrease. Gear alignment and bearing rigidity impact the effective face width, which may be affected by bearing clearances and misalignments in couplings between the driving and driven shafts (e.g., in jaw couplings). To address the variation in load distribution due to these factors, a full system approach should be adopted. However, a comprehensive study of these effects is beyond the scope of the current work. In statistical approach, this can be accounted for by considering the minimum value of face width. To understand this, let us consider mean value of width as m_c and standard deviation as s_c . In the statistical approach, the minimum value of face width will be $m_c - 3s_c$. Considering this, there is no need to account for K_m and standard deviation in face width. In statistical approach, variation in material properties is accounted. In addition, the minimum possible value of face width is considered. Therefore, there is no need to account for size factor K_s . There is a very rare chance of designing thin rim of gear.

which is a function of the gear's tooth thickness and meshing point radius at the meshing point. While the module (m), number of teeth (Z_p), and nominal pressure angle (ϕ_{nom}) remain constant once chosen, wear or manufacturing errors may cause deviations from the ideal profile, leading to a non-ideal pressure angle. Consequently, I become a function of the instantaneous pressure angle ϕ . As the Young's modulus and poisson's ratio will remain constant, the C_p value shall also be considered constant.

The standard deviation of Equation (11) is estimated by Equation (12):

The mean value (μ_σ) of stresses is obtained by substituting the mean value of each variable given in Equation (1), and values are tabulated in the Table 6.

To incorporate the probabilistic approach, the coefficient of variation (COV) is examined through the experiment, which indicates precision processing of material and geometry. As per the experimental setup present, it has been observed that speed is set to 2000 R.P.M. then it fluctuates ± 20 R.P.M. while torque is set to 100 Nm, it used to fluctuate the ± 1 Nm. For geometrical specification, visual measuring machine (V.M.M.) is used, as shown in Figure 6. It has been observed that the outer diameter standard deviation is 0.054 mm, and face width is 0.02 mm. Since the pitch circle diameter is hypothetical, we can assume that whatever the standard deviation of outer diameter, it will be the same pitch circle diameter. For the

The case study discussed in the previous section is considered to examine the variation of solutions without statistical variation obtained using AGMA Equation (1) and FEM result.

instantaneous pressure angle, the tooth thickness is measured using gear tooth vernier. Based on that, the instantaneous pressure angle at pitch circle is deviated with a standard deviation of 0.03 degree. The standard deviation for different variables T, F, D and N are $\sigma_T=0.33$ Nm, $\sigma_F=0.02$ mm, $\sigma_D=0.054$ mm, $\sigma_\theta=0.04$ degree and $\sigma_N=6.66$ rpm respectively. To perform partial differentiation of Equation (12), numerical method was adopted using MATLAB®, and codes are given in Appendix C. In this case, the reliability of the pinion is estimated.

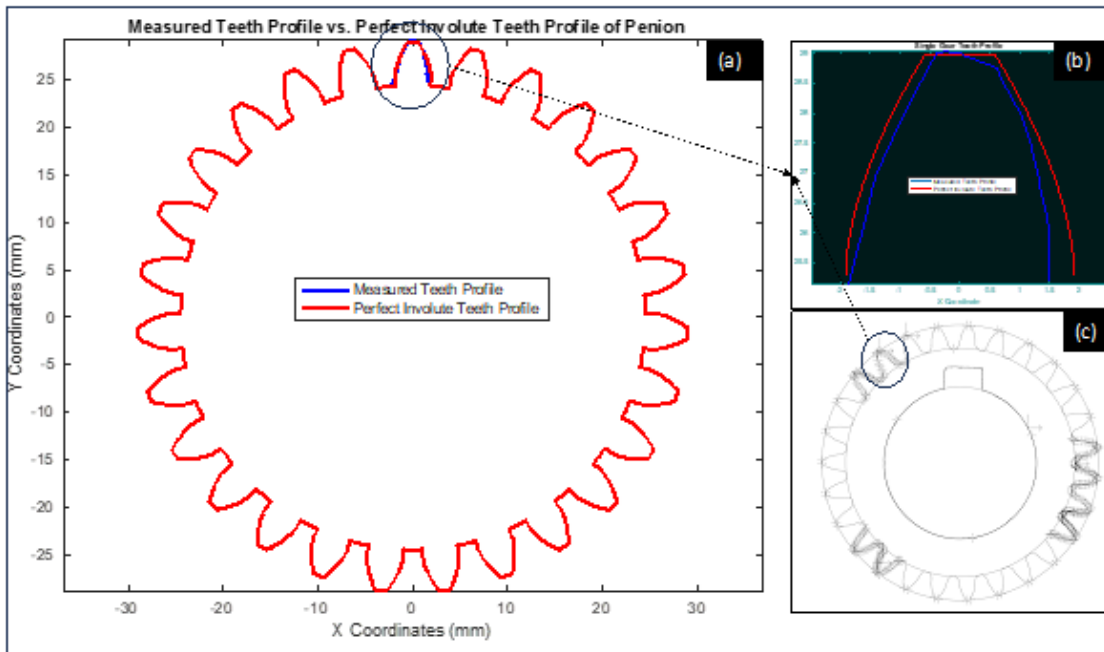


Figure 6. Deviation between theoretically generated involute gear profile (a), enlarged subsection (b) and experimentally measured profile by V.M.M. (c) teeth profile

To determine the probability of survival under contact fatigue, it is required to estimate the standard deviation of the contact stress. For that purpose, one needs to find values of the following partial differential terms. Substituting these values in Equation (12), the estimated value of μ_{σ_c} is 898 MPa and σ_{σ_c} is 143.59 MPa. The mean (μ_{s_y}) and standard deviation (σ_{s_y}) of the allowable pitting strength is estimated to be 1250 MPa and 50 MPa respectively. The mean value (μ_Q) of the contact stress value is 352 MPa. The normalized factor ‘Z’ is:

$$Z = -\frac{1250 - 898}{\sqrt{143.59^2 + 50^2}} = -2.31$$

The reliability value corresponding to value of -1.35 is estimated as $(1 - 0.0107) = 0.9893$. In other words, there are ~1.07% chances of pinion failure.

3. CONCLUSIONS

The classical gear design approaches (AGMA) are deterministic in nature, and do not incorporate variations in parameters. Gears designed for contact stresses using the AGMA method require several subjective design correction factors. Similarly gear designed using the finite element method is complex, and the inclusion of errors would be for specific illustration. Therefore, in the present work a robust probabilistic approach has been proposed which includes all the variation in the parameters and is easy to implement. This approach reduces subjectivity by eliminating correction design factors and provides more realistic results.

The gear and pinion were designed using probabilistic, and AGMA proposed approaches, and the result was compared with the FEM results. Following conclusions were derived from different approaches:

- (i) AGMA approach: Both pinion and gear in contact conditions were safe.
- (ii) Established FEM approach: Pinion showed chances of failure in contact fatigue (factor of safety is lesser than 1).
- (iii) Proposed probabilistic approach: 1.07 % chances of failure in pinion due to contact fatigue.

Authors' Contributions

Conceptualization, H.H.; Methodology, H.H.; Resources, Y.C., K.N.S.; Supervision, H.H.; Writing-editing of the manuscript K.N.S., Y.C.; Data curation, K.N.S., and Y.C.; formal analysis, K.N.S.; FEM analysis, Y.C.; writing—original draft preparation, K.N.S. All authors have read and agreed to the published version of the manuscript.

Funding: This research received no external funding.

Data Availability Statement: Data can be shared on request.

Conflicts of Interest: The authors declare no known conflicts of interest.

Appendix

A1. Calculation for various factor AGMA Pitting Resistance Equation

As per the current AGMA standards K_v is represented as:

$$K_v = \left(\frac{A + \sqrt{\frac{V}{1000}}}{A} \right)^B \quad (A.1)$$

$$A=5.56; B=0.5 \quad (A.2)$$

Where Q_v is the quality factor.

In case of Pinion, Speed is 2000 R.P.M., then K_v using Equation (A.1 and A.2) = 1.1949

In case of Gear, Speed is 1018.86 RPM, then K_v using Equation (A.1 and A.2) = 1.1949

Table A.1 Table of overload Factor

Power Source/Load	Uniform	Moderate shock	Heavy Shock
Uniform	1	1.25	1.75
Light Shock	1.25	1.5	2
Medium Shock	1.5	1.75	2.25

The overload factor, K_o , accounts for the degree of non-uniformity in driving torques. The table for the overload factor is given in table 1 in appendix. Since in our case load is done using dynamometer and there is some fluctuation in torque will result in light shock and motor also give some fluctuation in R.P.M. that will also lead to light/ moderate shock then we can

choose the $K_m=1.5$. The size factor, K_s , reflects dependence of stress on the size of gear. The size factor may be taken as unity for most gears, provided a proper choice of steel is made for the size of the part and its heat treatment and hardening process.

The load distribution factor, K_m , accounts for the non-uniformity in distribution of load across the line of contact. The load factor value is determined by Equation (A.4).

$$K_m = 1 + C_{mc}(C_{pf}C_{pm} + C_{ma}C_e) \tag{A.4}$$

Where,

$$C_{mc} = \begin{cases} 1 & \text{For uncrowned teeth} \\ 0.8 & \text{For crowned teeth} \end{cases} \tag{A.5}$$

Crowning is not provided for any gear. Hence, C_{mc} is 1.

If $F/(10d) < 0.05$, $F/(10d) = 0.05$ is used,

$$C_{pm} = \begin{cases} 1 & \text{For straddle mounted pinion with } S_1/S < 0.175 \\ 0.8FF & \text{For straddle mounted pinion with } S_1/S \geq 0.175 \end{cases} \tag{A.6}$$

S is the center distance between two bearings and S_1 is the distance between the center line of the gear face and mid-point of shaft-system as shown in Figure A1. In our case the value of S_1 is zero so we can choose $C_{pm} = 1$

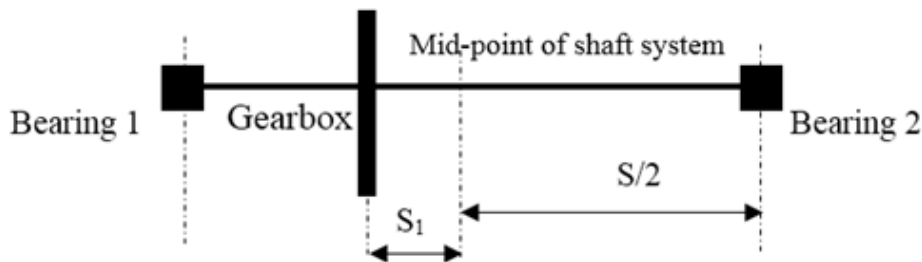


Figure A.1. Definition of distance S and S_1 used in evaluation C_{pm}

$C_{ma} = A + BF + CF^2$, the value of A , B , and C is given in Table A.2.

Table A.2 Empirical Constants A , B , and C to find C_{ma}

Condition	A	B	C
Open gearing	0.247	6.57×10^{-4}	-3.01×10^{-6}
Commercial, enclosed units	0.127	6.22×10^{-4}	-3.66×10^{-6}
Precision, enclosed units	0.0675	5.03×10^{-4}	-3.65×10^{-6}
Extra precision enclosed gear units	0.0036	4.02×10^{-4}	-3.24×10^{-6}

Based on values of A , B , C for Precision, enclosed units in our case, C_{ma} is for pinion and gear is 0.0801

$$C_e = \begin{cases} 0.8 & \text{For gearing, compatibility is improved by lapping or both} \\ 1 & \text{For all other conditions.} \end{cases} \tag{A.7}$$

Since no lapping is done on both the gear, so we can select the $C_e=1$

$$C_{pf} = \begin{cases} \frac{F}{10d} - 0.025 & F < 25mm \\ \frac{F}{10d} - 0.0375 + F4.92 \times 10^{-4} & 25mm < F < 425mm \\ \frac{F}{10d} - 0.1109 + F8.15 \times 10^{-4} - F^23.53 \times 10^{-4} & 425mm < F < 1000mm \end{cases} \quad (A.8)$$

For face width 33 mm, enclosed units in our case based on Equation (A.8), C_{ma} is for pinion and gear is 0.05 and 0.0398 respectively.

So finally, K_m for pinion will be 1.12 and for gear it is found 1.1301 based on Equation (A.4) to (A.8).

The surface condition factor C_f is used only in the pitting resistance Equation, it depends on Surface finish as affected by, but not limited to, cutting, shaving, lapping, grinding, shot peening, residual stress and plastic effects (work hardening).

Appendix B. Calculation for Corrected Fatigue Strength Equation

C_H is calculated by Equation B.1. For through-hardened pinions running against through hardened gears, it is expressed as:

$$C_H = 1 + A(m_G - 1) \quad (B.1)$$

Where m_G is the gear ratio, A is the calculated using the following conditions:

$$\begin{cases} \text{if } \frac{HB_p}{HB_g} < 1.2 \text{ then } A = 0 \\ \text{if } 1.2 < \frac{HB_p}{HB_g} < 1.7 \text{ then } A = 0.00898 \frac{HB_p}{HB_g} - 0.00829 \\ \text{if } \frac{HB_p}{HB_g} > 1.7 \text{ then } A = 0.00698 \end{cases} \quad (B.2)$$

In our case, both gears are of similar hardness and C_H is unity. In this case, C_L for pinion and gear is 0.907 from AGMA 2001-D04.

Table B.1 Reliability factor as per AGMA standard

Requirement	C_R
Fewer than one failure in 10,000	1.50
Fewer than one failure in 1,000	1.25
Fewer than one failure in 100	1.00
Fewer than one failure in 10	0.852
Fewer than one failure in 2	0.702

Appendix C. MATLAB Code For Standard Deviation Of Contact Stress

```

clc;
close all;
clear all;
% Constants
C_P = 191.64; % Elastic coefficient
K_o = 1.5; % load factor
C_f = 1; % surface finish factor
K_m = 1.12; % load distribution factor
K_s = 1.1; % size factor
Zp=27; % number of theeth on pinion
Zg=53; % number of theeth on gear
% Standard deviations for each variable
sigma_T = 0.33; % Nm
sigma_F = 0.02; % mm
sigma_D = 0.054; % mm
sigma_phi = 0.04; % degrees
sigma_N = 6.66; % RPM
% Symbolic variables (uncertain variables)
syms D T F N phi
%intermediate equations variables
syms w_t Ft I
% Velocities and coefficients
V = pi * D * N / 60; % Velocity mm/s
w_t = 2 * T / D; % Tangential load N
Ft = w_t / F; % Transmitted load per unit width (N/mm)
I = ((sin(phi) * cos(phi)) / 2)*Zp/(Zg+Zp); % Example
expression for I
% Define K_v
K_v=sqrt((5.56+sqrt(V/1000))/5.56); % Dynamic factor
% Contact stress equation
sigma_c = C_P * sqrt((Ft * K_o * C_f * K_m * K_s *
K_v) / I*D);
% Partial derivatives
d_sigma_c_D = diff(sigma_c, D);
d_sigma_c_T = diff(sigma_c, T);
d_sigma_c_F = diff(sigma_c, F);
d_sigma_c_N = diff(sigma_c, N);

```

```

d_sigma_c_phi = diff(sigma_c, phi);
% Substitute mean values into the partial derivatives
mean_D = 54; % mm (avg pitch circle diameter)
mean_T = 100; % Nm (Avg torque)
mean_F = 33; % mm (face width)
mean_N = 2000; % R.P.M. (speed of pinion)
mean_phi = deg2rad(20); % Convert degrees to radians
(pressure angle)
% Substitution in derivatives
d_sigma_c_D_val = subs(d_sigma_c_D, [D, T, F, N,
phi], [mean_D, mean_T, mean_F, mean_N, mean_phi]);
d_sigma_c_T_val = subs(d_sigma_c_T, [D, T, F, N,
phi], [mean_D, mean_T, mean_F, mean_N, mean_phi]);
d_sigma_c_F_val = subs(d_sigma_c_F, [D, T, F, N,
phi], [mean_D, mean_T, mean_F, mean_N, mean_phi]);
d_sigma_c_N_val = subs(d_sigma_c_N, [D, T, F, N,
phi], [mean_D, mean_T, mean_F, mean_N, mean_phi]);
d_sigma_c_phi_val = subs(d_sigma_c_phi, [D, T, F, N,
phi], [mean_D, mean_T, mean_F, mean_N, mean_phi]);
% Substituting into the variance calculation
sigma_c_variance_expr = sqrt(...
(d_sigma_c_D_val * sigma_D)^2 + ...
(d_sigma_c_T_val * sigma_T)^2 + ...
(d_sigma_c_F_val * sigma_F)^2 + ...
(d_sigma_c_N_val * sigma_N)^2 + ...
(d_sigma_c_phi_val * sigma_phi)^2);
% Convert to double
sigma_c_variance = double(sigma_c_variance_expr);
% Display result
disp(['Variance of sigma_c: ',
num2str(sigma_c_variance)]);

```

References

- [1] Shigley, J. E., Mitchell, L. D., & Saunders, H. (1985). Mechanical engineering design.
- [2] Stoker, K., Chaudhuri, A., & Kim, N. H. (2010, January). Safety of spur gear design under non-ideal conditions with uncertainty. In *International Design Engineering Technical Conferences and Computers and Information in Engineering Conference* (Vol. 44090, pp. 69-79).
- [3] Jangra, D., Hirani, H., & Darpe, A. K. (2023). Effect of combined (radial-axial-angular direction) misalignment on sliding wear of spur gears: A comprehensive study. *Tribology International*, 189, 108908.
- [4] Kumar, P., Hirani, H., & Agrawal, A. (2017). Fatigue failure prediction in spur gear pair using AGMA approach. *Materials Today: Proceedings*, 4(2), 2470-2477.
- [5] Jangra, D., & Hirani, H. (2024). A Comparative Study of Wear Debris and Vibration-Based Gear Damage Detection Methods Applied to Mild Wear in a Spur Gear System. *Journal of Vibration Engineering & Technologies*, 1-11
- [6] Jebur, A. K., Khan, I. A., & Nath, Y. (2011). Numerical and experimental dynamic contact of rotating spur gear. *Modern Applied Science*, 5(2), 254.
- [7] Loc, N. H., & Anh, L. T. (2021, March). Contact stress analysis and optimization of spur gears. In *I.O.P. Conference Series: Materials Science and Engineering* (Vol. 1109, No. 1, p. 012004). I.O.P. Publishing.
- [8] Hirani, H., Jangra, D., & Sidh, K. N. (2023). Experimental Analysis of Chemically Degraded Lubricant's Impact on Spur Gear Wear. *Lubricants*, 11(5), 201.
- [9] J. J. Coy, D. P. Townsend, E. V. Zaretsky, *Dynamic Capacity and Surface Fatigue Life for Spur and Helical Gears*, J. Tribol. Vol. 98, No. 2, pp. 267-274, 1976.
- [10] Kumar, P., Hirani, H., & Agrawal, A. K. (2019). Effect of gear misalignment on contact area: Theoretical and experimental studies. *Measurement*, 132, 359-368.
- [11] Cameron, Z. A., & Krantz, T. L. (2023). Statistical distribution of gear surface fatigue lives at high reliability. *International Journal of Fatigue*, 167, 107350.
- [12] Haefner, B., & Lanza, G. (2017). Function-oriented measurements and uncertainty evaluation of micro-gears for lifetime prognosis. *CIRP annals*, 66(1), 475-478.
- [13] Hammouri, H. M., Sabo, R. T., Alsaadawi, R., & Kheirallah, K. A. (2020). Handling skewed data: A comparison of two popular methods. *Applied Sciences*, 10(18), 6247.
- [14] Al-Tubi, I., H. Long, P. Tavner, B. Shaw, J. Zhang. *Probabilistic analysis of gear flank micro-pitting risk in wind turbine gearbox using supervisory control and data acquisition data*, I.E.T. Renewable Power Generation, pp. 1-5, 2015.
- [15] B.P. Gautham, P. Gupta, N.H. Kulkarni, J.H Panchal, J.K. Allen, F. Mistree, *Robust Design of Gears With Material and Load Uncertainties*, In ASME 2013 International Design Engineering Technical Conferences and Computers and Information in Engineering Conference (pp. V03BT03A046-V03BT03A04, 2013).
- [16] El-Sayed S. Aziz, C. Chassapis, *Probabilistic Simulation Approach to Evaluate the Tooth-Root Strength of Spur Gears with FEM-Based Verification*, Engineering, Vol. 3 No. 12, pp. 1137-1148, 2011.
- [17] X. Q. Peng, Liu Geng, Wu Liyan, G. R. Liu, K. Y. Lam, *A stochastic finite element method for fatigue reliability analysis of gear teeth subjected to bending*, Computational Mechanics, Vol. 21, No. 3, pp. 253-261, 1998.
- [18] Li Shuting, *Finite element analyses for contact strength and bending strength of a pair of spur gears with machining errors, assembly errors and tooth modifications*. Mechanism and Machine Theory, Vol. 42, pp.88–114, 2007.
- [19] Li. Shuting, *Effects of machining errors, assembly errors and tooth modifications on loading capacity, load-sharing ratio and transmission error of a pair of spur gears*, Mechanism and Machine Theory, Vol. 42, pp.698–726, 2007.
- [20] J.D. Andrews, *A Finite Element Analysis of Bending Stresses Induced in External and Internal Involute Spur Gears*, Journal of Strain Analysis, IMechE, Vol. 26, No.3, 1991.
- [21] J. Kramberger, M. Sraml, Potrc, J. Flaker, *Numerical calculation of bending fatigue life of thin-rim spur gears*, Engineering Fracture Mechanics, Vol. 71, pp. 647–656, 2004.
- [22] Chen, Z., Jiang, Y., Li, S., Tong, Z., Tong, S., & Tang, N. (2023). Uncertainty propagation of correlated lubricant properties in gear tribodynamic system. *Tribology International*, 179, 107812.
- [23] S. Glodez, M. Sraml, J. Kramberger, *A computational model for determination of service life of gears*, International Journal of Fatigue, Vol. 24, pp. 1013–1020, 2002.
- [24] Khudhair, M. R. (2020). Design and Analysis for Spur Gear by Using AGMA Standards and F.E.A.: A Comparative Study.
- [25] Houser, D. R., Harianto, J., Chandrasekaran, B., Josephson, J., & Iyer, N. (2000, September). A multi-variable approach to determine the “Best” gear design. In *International Design Engineering Technical Conferences and Computers and Information in Engineering Conference* (Vol. 35166, pp. 31-39). American Society of Mechanical Engineers.
- [26] Guerine, A., Hami, A. E., Walha, L., Fakhfakh, T., & Haddar, M. (2016). Dynamic response of a spur gear

- system with uncertain parameters. *Journal of Theoretical and Applied Mechanics*, 54(3), 1039-1049.
- [27] R.G. Budynas, J.K. Nisbett, “*Mechanical Engineering Design*, Indian edition, The McGraw-Hill Companies, Inc., New York, 2014.
- [28] Franco, R. R., de Souza, G. F., & da Silva, C. H. (2018, January). Experimental uncertainty analysis of gear fatigue life theoretical prediction. In 2018 Annual Reliability and Maintainability Symposium (RAMS) (pp. 1-7). IEEE.
- [29] Alemayehu, F. M., & Ekwaro-Osire, S. (2013). Uncertainty considerations in the dynamic loading and failure of spur gear pairs. *Journal of Mechanical Design*, 135(8), 084501
- [30] Y. A. Tesfahunegn, F. Rosa, C. Gorla, *The effects of the shape of tooth profile modifications on the transmission error, bending, and contact stress of spur gears*, Proc. IMechE Part C: J. Mechanical Engineering Science, Vol. 224, 2009.
- [31] Dantan, J. Y., Vincent, J. P., Goch, G., & Mathieu, L. (2010). Correlation uncertainty—Application to gear conformity. *CIRP annals*, 59(1), 509-512.
- [32] Iso, I., & OIML, B. (1995). *Guide to the Expression of Uncertainty in Measurement*. Geneva, Switzerland, 122, 16-17.